



## OPEN Exploring the mechanisms of chronic obstructive pulmonary disease and Crohn's disease: a bioinformatics-based study

Xinxin Zhang<sup>1</sup>, Caiping Liu<sup>1</sup>, Luqian Cao<sup>1</sup>, Hongguang Tang<sup>1</sup>, Haiyun Jiang<sup>1</sup>, Changjing Hu<sup>1</sup>, Xuehong Dong<sup>1</sup>, Feiyang Zhou<sup>1</sup>, Kunming Qin<sup>1</sup>, Qiang Liu<sup>1</sup>, Jinyang Shen<sup>1</sup>✉ & Yue Zhou<sup>2</sup>✉

This study explored the comorbid mechanisms between Crohn's disease (CD) and chronic obstructive pulmonary disease (COPD) using bioinformatics analysis. From the Gene Expression Omnibus (GEO) microarray dataset, 349 common differentially expressed genes (coDEGs) were identified, and 8 shared hub genes were found: CCL2, CXCL1, TLR2, ICAM1, PTPRC, ITGAX, PTGS2, and MMP9, which were vital for immune function and regulation of inflammatory responses. In addition, the study also analyzed the association between coDEGs and immune cell infiltration using the single-sample gene set enrichment algorithm (ssGSEA). Potential drugs related to these genes were identified using the connectivity map (CMap). These findings provided new perspectives for understanding the interaction between CD and COPD.

**Keywords** Crohn's disease, Chronic obstructive pulmonary disease, Bioinformatics analysis, Single-sample gene set enrichment algorithm, Connectivity map

Chronic obstructive pulmonary disease (COPD) is the leading cause of death among chronic lung diseases, ranking third globally, with increasing morbidity and mortality rates<sup>1</sup>. COPD is characterized by persistent respiratory symptoms and progressive airflow obstruction<sup>2</sup>. Studies show that COPD is significantly more lethal than asthma, with a mortality rate about eight times higher<sup>3</sup>. According to the latest epidemiological projections, the overall prevalence of COPD and mortality is expected to increase by 8% by 2030<sup>4</sup>. COPD pathogenesis arises from multiple factors, including smoking, genetics, oxidative stress, and inflammation<sup>5-7</sup>. With the increasing research on the pathogenesis of COPD, multiple biological processes such as cellular senescence and immune imbalance are now covered<sup>8,9</sup>. Studies have found that gut microbiota imbalances are prevalent in the COPD patient population<sup>10</sup>.

Crohn's disease (CD) is a chronic inflammatory bowel disease affecting the gastrointestinal tract, causing abdominal pain, diarrhoea, weight loss, and other symptoms<sup>11,12</sup>. The main pathogenesis of Crohn's disease includes immune dysregulation, intestinal barrier dysfunction, and intestinal microbial imbalance<sup>13,14</sup>. Genetics, environmental factors, and alterations in gut microbiota are thought to influence the risk of developing and worsening CD<sup>15</sup>. Furthermore, the mesenteric lymphatic system connects the gut and lungs, enabling bacteria, their fragments, or metabolites to cross the intestinal barrier and enter systemic circulation, affecting the pulmonary immune response<sup>16</sup>. Previous studies found that patients with CD had an increased risk of causing death from COPD<sup>17</sup>. The comorbidity rate of CD also tends to be higher in patients with COPD<sup>18,19</sup>.

Recent studies suggest a potential link between the lung and gut environments in COPD, indicating that these organ systems may interact. This has heightened interest in the complex interactions among the host, microbial communities, and respiratory disease<sup>20</sup>. It had been shown that gut microbiota imbalance might modulate the TLR4/NF- $\kappa$ B signalling pathway in the pulmonary immune system, activate pulmonary oxidative stress, and mediate lung injury by modulating the intestinal barrier<sup>21</sup>. According to Budden et al.<sup>22</sup>, bidirectional communication between the gut and lungs played a crucial role in the development and progression of COPD.

<sup>1</sup>Department of Pharmacy, Jiangsu Ocean University, 59 Cangwu Road, Haizhou District, Lianyungang 222000, Jiangsu, China. <sup>2</sup>Department of Pharmacy, Lianyungang Affiliated Hospital of Nanjing University of Chinese Medicine, No. 160, Chaoyang Middle Road, Haizhou District, Lianyungang 222004, Jiangsu, China. ✉email: shenjy@jou.edu.cn; zhouy367@outlook.com

Mahmud et al.<sup>23</sup> used bioinformatics and systems biology to identify shared molecular pathways and biomarkers among COPD, IPF, and COVID-19, indicating that patients with these chronic lung diseases may face a higher risk of COVID-19 infection.

Huang et al.<sup>24</sup> used bioinformatics to identify immune cell infiltration and potential diagnostic biomarkers for CD.

Despite evidence indicated that intestinal diseases were closely associated with COPD, the underlying mechanisms are unclear. Further research is needed to explore their interactions. In this study, the connection between COPD and CD were investigated by searching for common differentially expressed genes (coDEGs) in COPD lung tissues and CD intestinal tissues with the help of bioinformatics technology. The identified shared gene signatures hold promise for elucidating biological mechanisms associated with the disease. In-depth exploration of these common biological pathways provided new perspectives for subsequent research and treatment.

## Results

### GSEA analysis in COPD and CD

In GSEA analysis, 165 pathways were enriched in COPD and 126 in CD, with 85 pathways common to both diseases (Supplementary 1). Immune response, infectious diseases, and signaling pathways were predominant. Enriched pathways in human diseases included leishmaniasis, systemic lupus erythematosus, malaria, tuberculosis, amoebiasis, and viral myocarditis (Fig. 1A,C). In bioorganic systems, pathways enriched for hematopoietic cell lineage, osteoclast differentiation, TNF signaling, toll-like receptor signaling, cytokine–cytokine receptor interaction, and NOD-like receptor signaling were identified, all related to the immune system (Fig. 1B,D).

### Identification of differentially expressed genes

2221 DEGs were identified between COPD patients and healthy controls according to the GSE148004 dataset (882 up regulated, 1339 down regulated) (Fig. 2A,C). In the GSE75214 dataset, 2338 DEGs were identified between CD patients and healthy controls (974 up regulated, 1364 down regulated) (Fig. 2B,D). Additionally, 349 coDEGs were shared between COPD and CD, with 81 up regulated and 268 down regulated coDEGs (Fig. 2E). This suggested that similarities in molecular mechanisms might exist between COPD and CD (Supplementary 2). Figure 3 showed the boxplots and PCA plots of COPD and CD. The absence of outliers in the boxplots for patient and normal samples indicated high quality.

### Functional enrichment analysis of CoDEGs

In order to understand the biological functions of shared genes, 349 coDEGs identified earlier were analyzed using GO and KEGG pathway annotation. The top 10 significantly different BP, CC and MF entries were identified

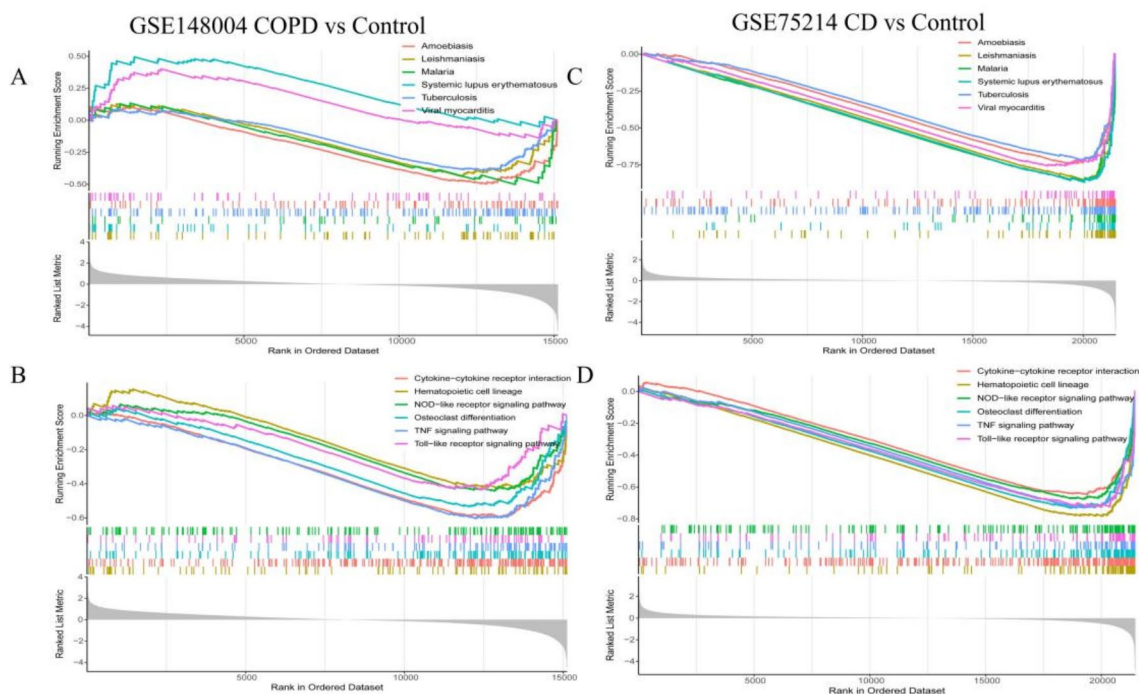


**Fig. 1.** GSEA analysis for GSE148004 (COPD) and GSE75214 (CD). (A,C) The genes of COPD and CD were both enriched in terms of human diseases. (B,D) The genes of COPD and CD were both enriched in terms of biological organic systems.

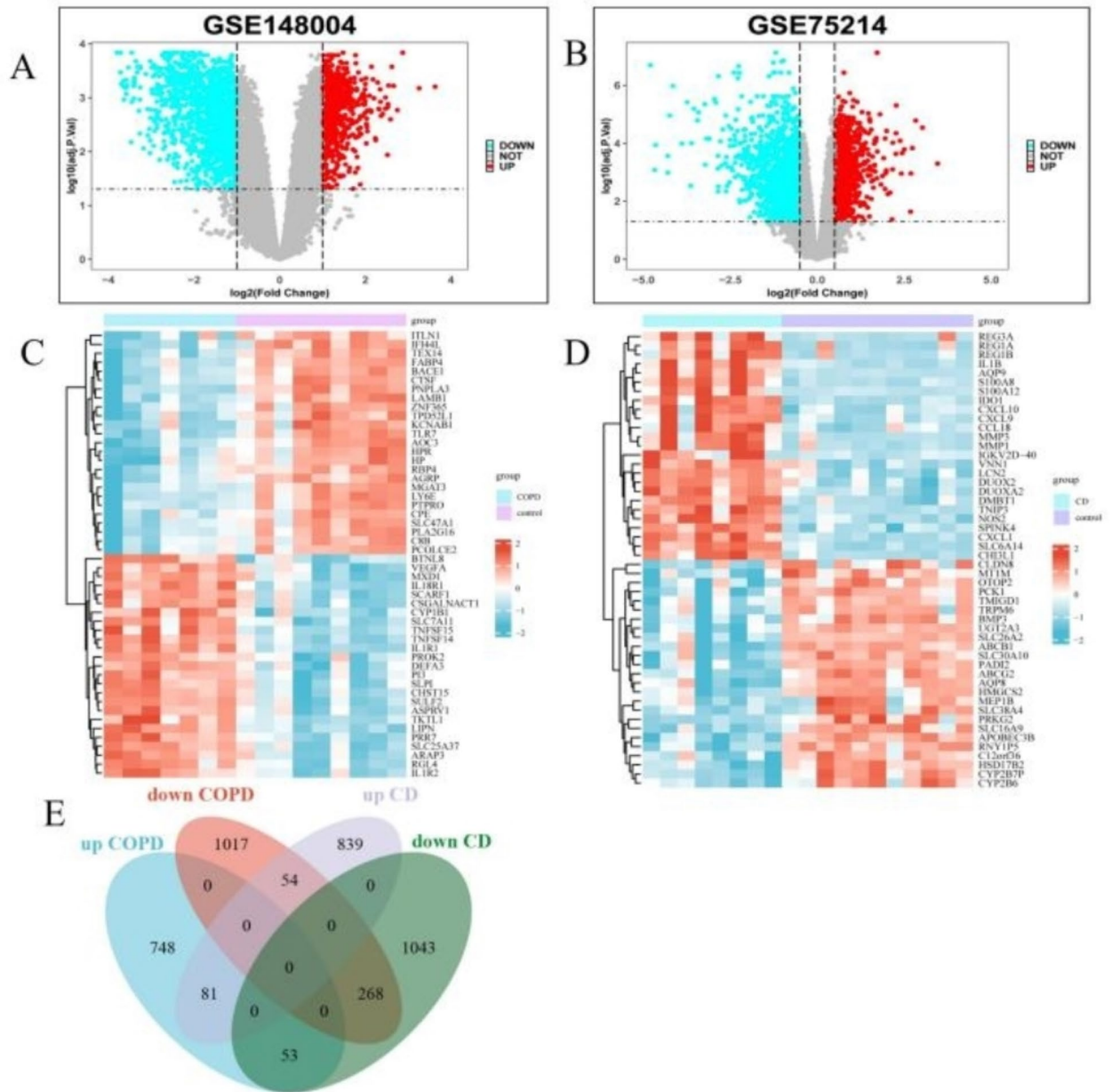


**Fig. 2.** CoDEGs in COPD and CD compared to control (healthy subjects). **(A)** Volcano plots of DEGs from GSE148004. **(B)** Volcano plots of DEGs from GSE75214. **(C)** Heatmap of DEGs from GSE148004, including 7 tissues from COPD and 9 tissues from healthy individuals. **(D)** Heatmap of DEGs from GSE75214, including 8 CD tissues and 11 healthy tissues. **(E)** Venn diagram of coDEGs extracted from DEGs of GSE148004 and GSE75214.

through GO analysis ( $P < 0.05$ ). Additionally, the top 10 significantly enriched pathways were annotated using KEGG ( $P < 0.05$ ).

GO/KEGG entries were mostly enriched and associated with immune responses. In the BP category, genes were mainly concentrated in positive regulation of cytokine production, regulation of inflammatory response, response to molecule of bacterial origin, positive regulation of defense response, response to lipopolysaccharide, leukocyte migration, cellular response to biotic stimulus, cellular response to molecule of bacterial origin, leukocyte apoptotic process and regulation of leukocyte apoptotic process. For the CC ontology, they were mainly enriched in pathways such as secretory granule membrane, tertiary granule and external side of plasma membrane. For MF ontology, they were mainly located in cytokine receptor activity, chemokine binding, cytokine binding and immune receptor activity (Fig. 4A). KEGG pathway was mainly located in the TNF signaling pathway, NF-kappa B signaling pathway, cytokine-cytokine receptor interaction, viral protein interaction with cytokine and cytokine receptor, C-type lectin receptor signaling pathway and B cell receptor signaling pathway.

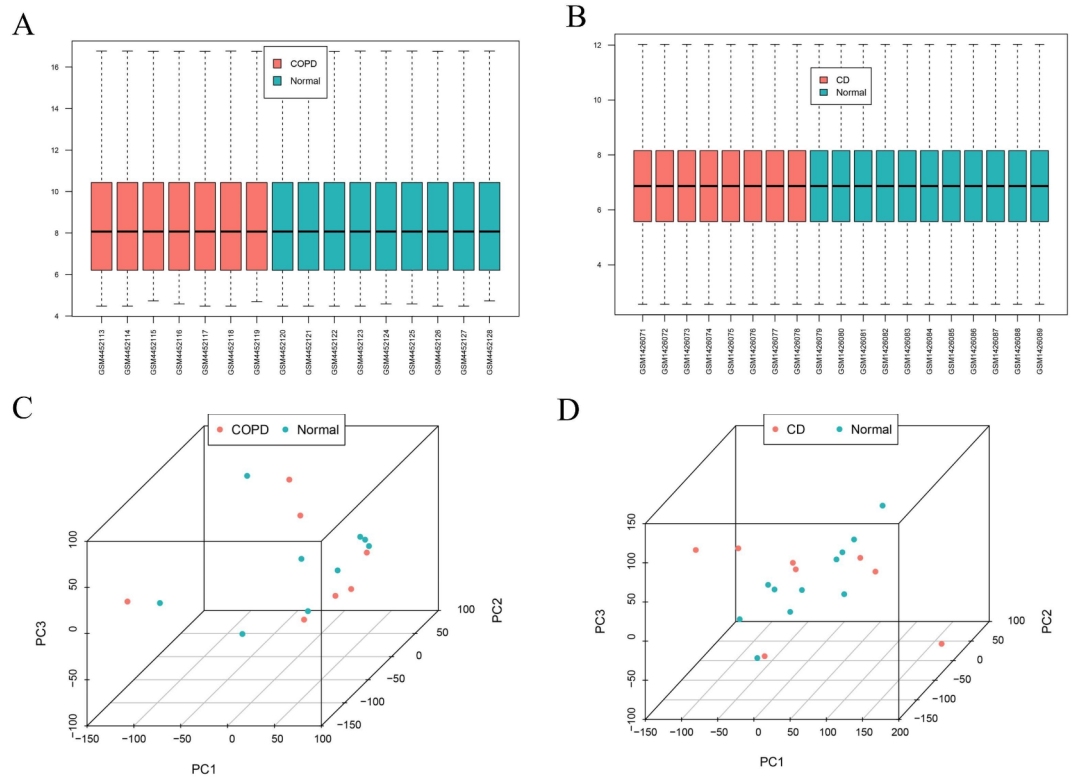


**Fig. 3.** Boxplots and PCA plots of COPD and CD datasets. **(A)** Boxplot of dataset GSE148004. **(B)** Boxplot of dataset GSE75214. **(C)** PCA diagram of dataset GSE148004. **(D)** PCA diagram of dataset GSE75214.

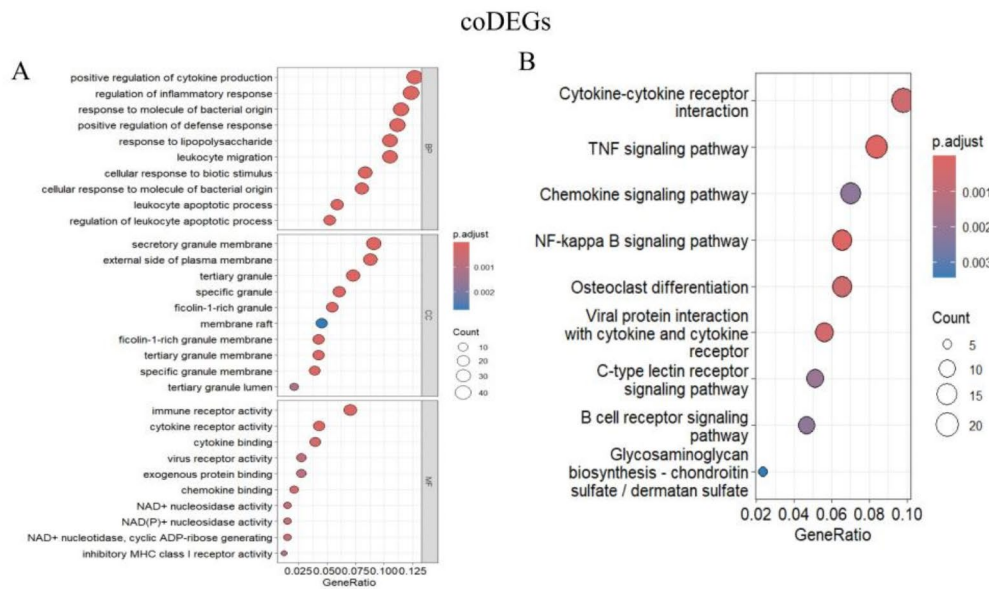


**Fig. 4.** Functional annotation for coDEGs. **(A)** Biological process, cellular component and molecular function. **(B)** KEGG analysis. The size of the circle represented the number of enriched genes, and the larger the circle, the more genes were enriched.

These pathways were closely related to immune responses, cell differentiation, and metabolic processes (Fig. 4B) (Supplementary Table 2).

### Construction of protein-protein interaction network of CoDEGs and acquisition of key gene modules

The 349 coDEGs analysed in the above steps were located in the PPI interaction network to further explore interactions between overlapping DEGs in the STRING database, with a total of 345 nodes and 1728 edges. Pink nodes were up regulated coDEGs and the blue nodes were down regulated coDEGs. Node sizes were scaled according to the degree value. The higher the node's degree, the higher the node's weight in the PPI network graph (Fig. 5A). The MCODE plug-in (<https://apps.cytoscape.org/apps/mcode>) was used to screen and analyze the key modules of PPI. Clusters with a Score greater than 4 were displayed, and a total of 4 clusters were screened. Cluster 1 included 24 nodes and 195 edges (Fig. 5B), featuring 1 up regulated gene and 23 down regulated genes. The identified pathways in GO enrichment were regulation of inflammatory response, chemokine-mediated signaling pathway, regulation of innate immune response, and regulation of adaptive immune response, all linked to inflammatory and immune responses. Cluster 2 consisted of 24 nodes and 76 edges (Fig. 5C), consisting of 1 up regulated gene and 23 down regulated genes. GO enrichment was associated with immune processes including leukocyte migration, regulation of leukocyte migration, myeloid leukocyte migration, immune receptor activity. Cluster 3 consisted of 5 nodes and 10 edges (Fig. 5D). GO enrichment was related to biosynthetic and metabolic pathways including chondroitin sulfate biosynthetic process, chondroitin sulfate proteoglycan biosynthetic process, proteoglycan metabolic process, and mucopolysaccharide metabolic process. Cluster 4 consisted of 7 nodes and 13 edges (Fig. 5E), and these pathways were mainly related to fatty acid metabolic process.

### CytoHubba central gene identification and functional enrichment analysis

Eight hub genes (CCL2, CXCL1, TLR2, ICAM1, PTPRC, ITGAX, PTGS2, and MMP9) were identified using the CytoHubba plug-in of Cytoscape software (Fig. 6A,B). GO and KEGG enrichment analysis of the hub genes yielded that biological processes (BP) was mainly focused on the immune response, including pathogen recognition, immune cell activation, inflammatory response to cell death. cellular components (CC) was primarily concentrated in cell granule-associated regions, associated with cell secretory function, signaling, and immune response. molecular functions (MF) was mainly involved in cell signaling, immune response, metabolic regulation, and intercellular communication ( $P < 0.05$ ) (Fig. 6C). KEGG analysis showed enrichment in pathways related to human diseases such as Rheumatoid arthritis, Malaria, Legionellosis, and Leishmaniasis ( $P < 0.05$ ) (Fig. 6D) (Supplementary 3).

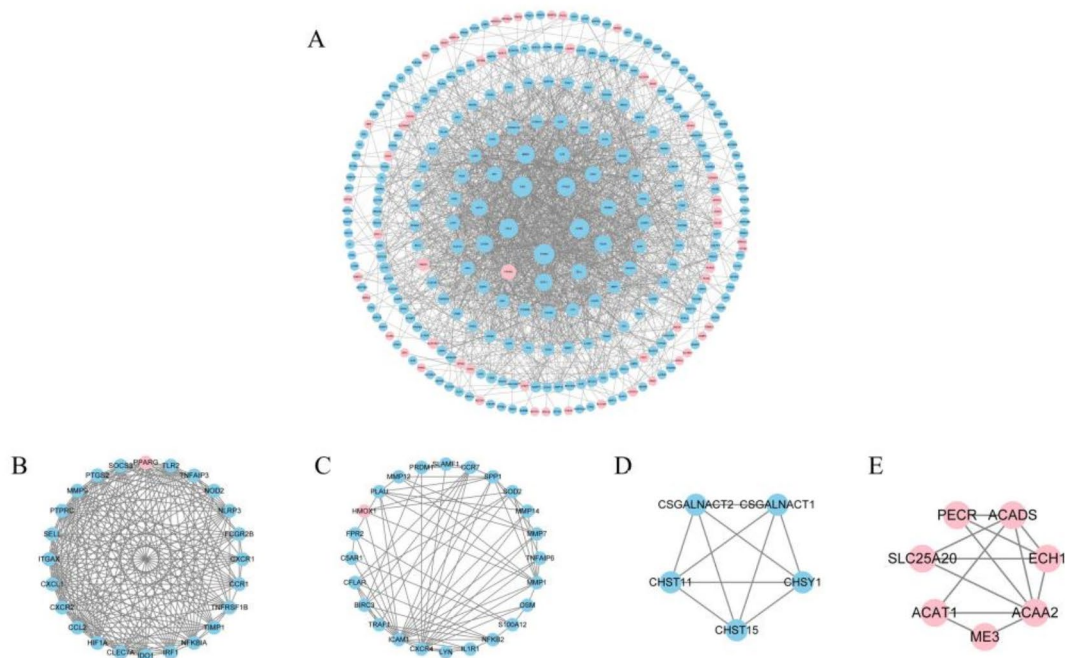


**Fig. 5.** Visualization of the PPI network and the important modules. (A) PPI network. (B–E) cluster 1–4.

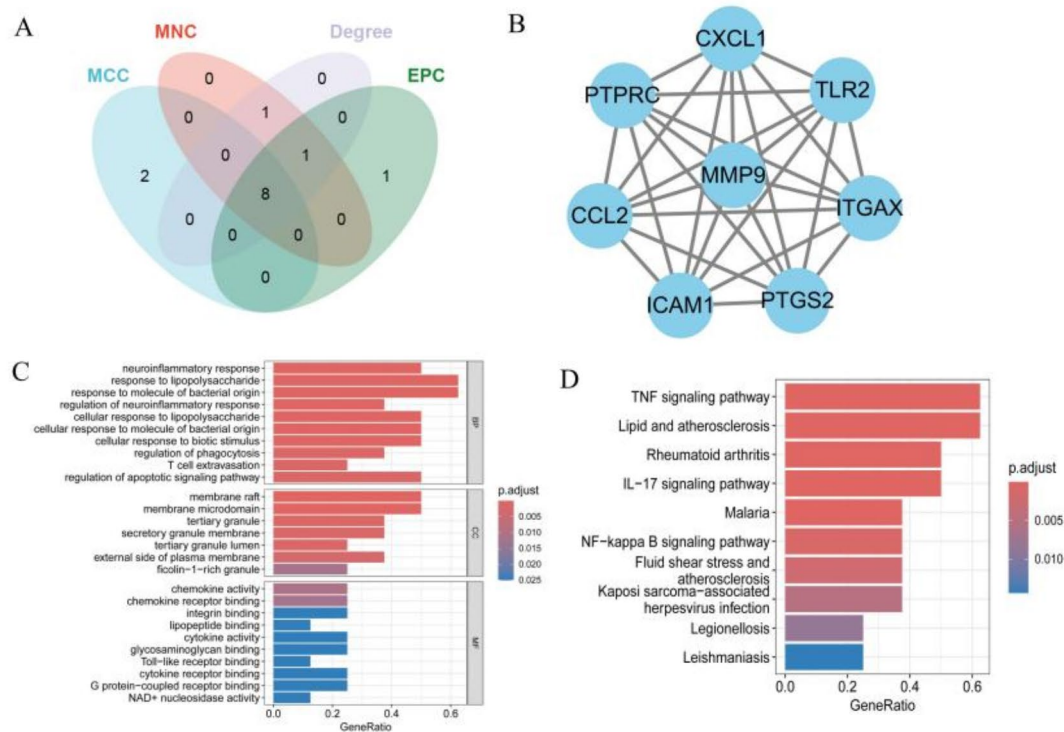


**Fig. 6.** Hub genes and functional enrichment analysis. **(A)** Hub genes formed four algorithms. **(B)** PPI network of hub genes. **(C)** GO enrichment analysis of hub genes. **(D)** KEGG enrichment analysis of hub genes.

### Validation of hub genes

The diagnostic potential of eight hub genes for COPD and CD diseases was evaluated through ROC analysis. In the COPD dataset, each of the eight hub genes had an area under the curve (AUC) exceeding 0.8413 for distinguishing patients from healthy controls (Fig. 7A). Similarly, in the CD dataset, the AUC values for the hub genes exceeded 0.8068 (Fig. 7B). The ROC curve analysis showed that the eight hub genes have potential value in predicting the risk of COPD and CD, offering a foundation for new targeted therapies for both diseases. To validate the accuracy and reliability of the findings, the expression levels of the eight hub genes were verified using the COPD and CD external validation datasets. The results revealed that the expression levels of gene TLR2 in the COPD dataset samples were significantly higher than those in the healthy control group (Fig. 7C,  $P < 0.05$ ). The expression levels of genes CCL2, CXCL1, ICAM1, ITGAX, and PTGS2 in the CD dataset samples were significantly higher than those in the healthy control group (Fig. 7D,  $P < 0.001$ ). These results suggest that these key genes could serve as powerful diagnostic biomarkers for predicting COPD and CD in patients (Supplementary 4). Figure 8 showed the boxplots and PCA plots of COPD and CD validation datasets. The absence of outliers in the boxplots for patient and normal samples indicated high quality.

### Assessment and visual analysis of immune infiltration

In this study, the ssGSEA algorithm was used to quantitatively analyze the distribution of relative infiltration levels (Fig. 9A,B) and assess the relative proportions (Fig. 10A,B) of 18 immune cells out of the 28 immune cells screened in the GSE148004 and GSE75214 datasets. Additionally, the correlation between 8 key hub genes and immune cell infiltration levels was systematically analyzed (Fig. 11A,B). These findings offered a foundation for a deeper understanding of the interaction of the gut-lung axis immune pathway in disease and healthy controls.

Compared to healthy controls, patients with COPD and CD showed significant differences in the distribution and proportion of various immune cells. In COPD, several immune cells were up regulated, including activated CD4 T cell, activated dendritic cell, plasmacytoid dendritic cell, natural killer cell, neutrophil, effector memory CD8 T cell, immature B cell, and eosinophil. Conversely, natural killer T cell, CD56dim natural killer cell, type 2 T helper cell, and regulatory T cell were down regulated in COPD. Some immune cells like central memory CD4 T cell, effector memory CD4 T cell, t follicular helper cell, myeloid derived suppressor cell, immature dendritic cell, and mast cell did not show statistically significant differences. In CD, up regulated immune cells included activated CD4 T cell, effector memory CD4 T cell, regulatory T cell, natural killer cell, myeloid derived suppressor cell, natural killer T cell, activated dendritic cell, immature dendritic cell, and mast cell. Conversely, effector memory CD8 T cell, type 2 T helper cell, CD56dim natural killer cell, plasmacytoid dendritic cell, and

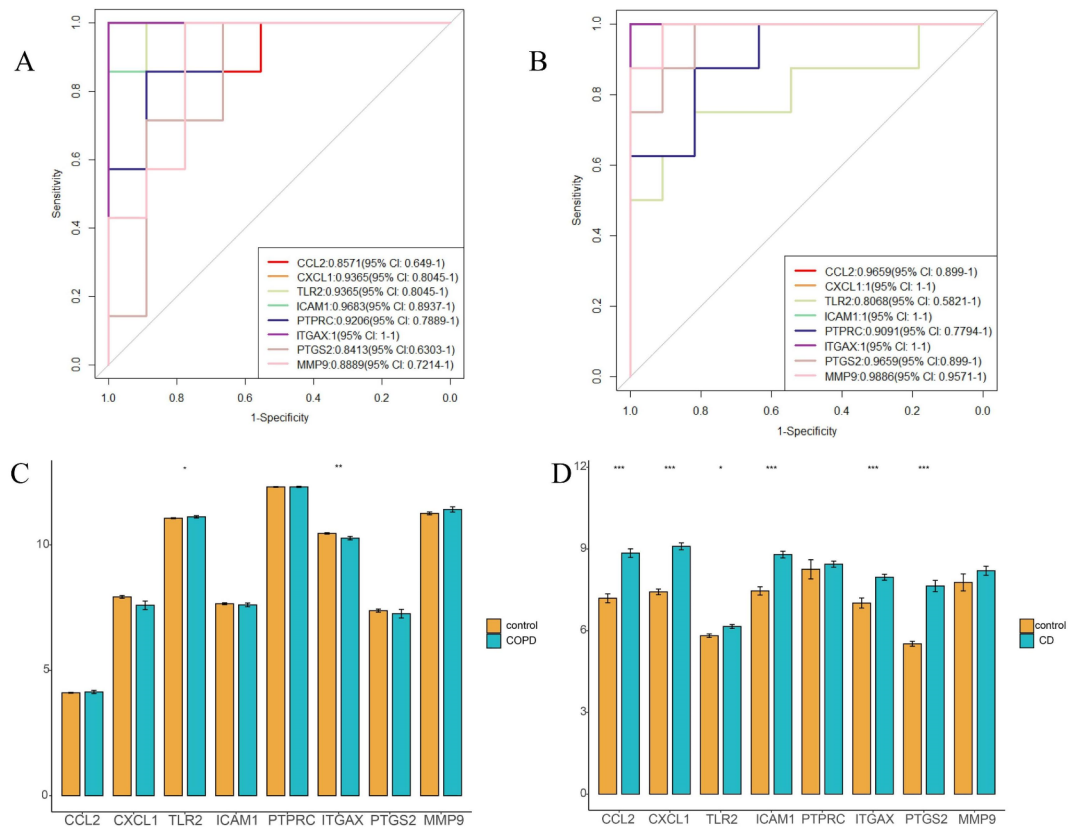


**Fig. 7.** ROC analysis and validation. **(A)** ROC curves of the hub genes in COPD. **(B)** ROC curves of the hub genes in CD. **(C)** Validation of expression values in COPD inflammation datasets. **(D)** Validation of expression levels in COPD inflammation datasets. This is a statistically significant marker, \* $P < 0.05$ , \*\* $P < 0.01$  and \*\*\* $P < 0.001$ .

eosinophil were down regulated in CD. Central memory CD4 T cell, T follicular helper cell, immature B cell, and neutrophil did not show statistically significant differences.

Biomarker analysis of 8 hub genes and infiltration analysis of 28 immune cells in COPD revealed a negative correlation between type 2 T helper cells and several hub genes, particularly CXCL1, TLR2, ICAM1, PTGS2, PTPRC, ITGAX, and MMP9 ( $P < 0.05$ ). Conversely, plasmacytoid dendritic cells showed a positive correlation with all hub genes ( $P < 0.05$ ), indicating enhanced immune cell infiltration in COPD.

Among the CD gene concentrations, all central genes showed significant negative correlations with CD56dim natural killer cells and effector memory CD8 T cells ( $P < 0.05$ ), and significant positive correlations with natural killer cells ( $P < 0.05$ ). These findings offer crucial evidence of immune pathways linking COPD and CD, highlighting the potential for exploring common pathogenesis and pharmacological targets through the lung-gut axis.

### CMap analysis reveals potential drugs based on common genetic features

In this study, we selected the top 10 up and down regulated genes from the coDEGs based on the  $|\log_2(\text{Fold Change})|$  for CMap analysis. The norm\_cs score predicted the top 10 potential drugs: RG-7388, irinotecan, orlistat, ryvidine, LE-135, ubenimex, JTC-801, puromycin, dapagliflozin, and ARRY-334,543 (Table 1). These drugs show potential as possible therapies for chronic obstructive pulmonary disease and Crohn's disease.

### Discussion

COPD is a common chronic respiratory disease with varying epidemiological characteristics varied among different age groups<sup>25</sup>. The gut microbiota plays a significant role in COPD, with a bidirectional interaction between the intestines and lungs that requires further study. Integrative bioinformatics analysis and machine learning tools were increasingly used to explore novel genes, potential diagnostic/prognostic biomarkers, underlying mechanisms, and therapeutic targets based on big data, shed light on diseases<sup>26,27</sup>. Research indicated a close relationship between chronic respiratory diseases like COPD, asthma, and idiopathic pulmonary fibrosis, and changes in gut microbiota composition<sup>28</sup>. Slyepchenko et al.<sup>29</sup> discussed that imbalances in the gut microbiota led to a series of complications, including the growth of harmful bacteria and increased intestinal permeability.

Genome-wide expression data analysis could enhance our understanding of disease mechanisms and provide a basis for studying the gut-lung axis system. The study identified 85 common pathways between GSE148004

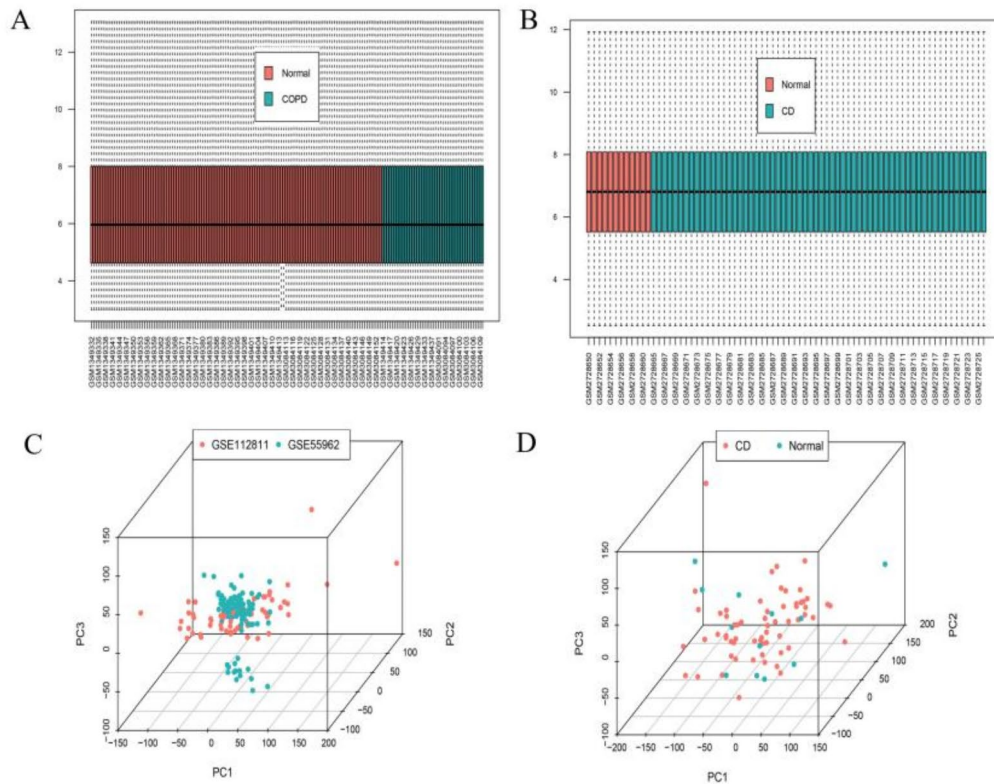


**Fig. 8.** Boxplots and PCA plots of COPD and CD validation dataset datasets. **(A)** Box line diagram for data sets GSE55962 and GSE112811. **(B)** Box line diagram for data set GSE102133. **(C)** PCA diagram for data sets GSE55962 and GSE112811. **(D)** PCA diagram for data set GSE102133.

(COPD) and GSE75214 (CD), mainly related to immune and infectious diseases, suggesting a potential link between the two conditions. Secondly, GO and KEGG enrichment analyses were performed on 349 selected coDEGs. GO analysis showed that BP functions were mainly concentrated in leukocyte-mediated immune responses, cytokine-mediated immune regulation, and molecular immunity to pathogens, while KEGG functional enrichment was mainly concentrated in pathogen recognition, immune cell activation, and regulation of immune responses. The study suggested that the mechanism linking COPD and CD might be closely related to the regulation of the immune system, especially in the regulation of immune and inflammatory responses. Some relevant studies had shown that gut microbes enhance resistance to bacterial infections in the lungs by modulating intestinal immune cells<sup>30</sup>. According to research, beneficial bacteria such as *Parabacteroides goldsteinii* could improve COPD symptoms by modulating the immune response<sup>31</sup>. To explore coDEGs in depth, eight shared hub genes were selected for GO/KEGG enrichment analysis. The BP functions of GO were mainly focused on including pathogen recognition, immune cell activation, and inflammatory response to cell death. After validating the hub genes' function, their significance were confirmed in patients with COPD and CD by analyzing the COPD versus CD validation dataset. Eight shared hub genes (CCL2, CXCL1, TLR2, ICAM1, PTPRC, ITGAX, PTGS2, and MMP9) were found to play a crucial role in both conditions. Since gut microbes can directly influence the characteristics of the immune system, immune activation might be the pathway through which gut microbes act on the respiratory system. Finally, 349 coDEGs were analysed for immune infiltration and immune relevance of 8 hub genes. The results further confirmed the association of coDEGs and hub genes between COPD and CD and the presence of 18 immune cells in the immune activity. This suggested that intestinal inflammatory diseases may impact respiratory function through specific immune systems, especially in relation to COPD. However, other potential factors required further exploration.

CCL2 belonged to the chemokine superfamily and exhibited higher expression in M2-polarized macrophages, while its receptor CCR2 was predominantly expressed on macrophages<sup>32,33</sup>. Studies had shown a significant link between high CCL2 levels and COPD. Elevated CCL2 encouraged monocyte accumulation in the lungs, increasing the number of macrophages and exacerbating lung inflammation in COPD<sup>34</sup>. CCL2 played a key regulatory role in inflammatory and immune responses by binding to the CCR2 receptor and activating cell signalling and migration<sup>35</sup>. In intestinal inflammation, CCL2 promotes the polarization of regulatory macrophages, exerting a protective effect that may be crucial in the pathogenesis of CD<sup>36</sup>. Carcinogens induced CXCL1 expression, promoting neutrophil recruitment and worsening the inflammatory response<sup>37</sup>. In COPD, alveolar macrophages increased secretion of inflammatory proteins, and cigarette smoke exposure exacerbates the release of these



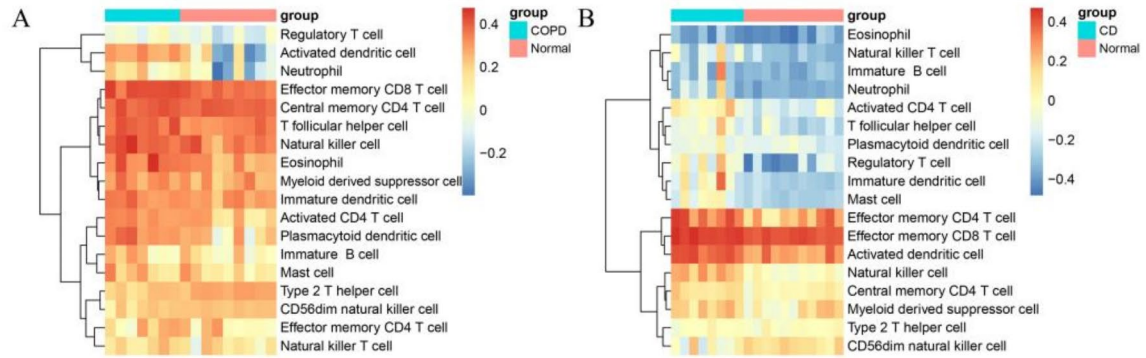


**Fig. 9.** Analysis of immune cell infiltration in COPD and CD. (A) Hierarchical clustering of the distribution of the 18 immune cells in COPD. (B) Hierarchical clustering of the distribution of the 18 immune cells in CD.

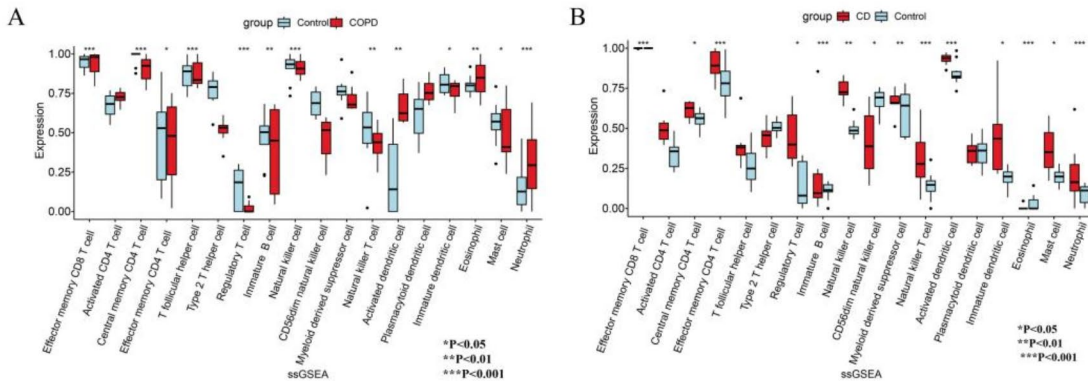


**Fig. 10.** Relative proportions of relative degrees of infiltration in COPD and CD. (A) Relative proportions in COPD. (B) Relative proportions in CD. This was a statistically significant marker: \* $P < 0.05$ , \*\* $P < 0.01$  and \*\*\* $P < 0.001$ .

mediators<sup>38</sup>. TLR2 was type I transmembrane receptor expressed on the cell surface<sup>39</sup>. The association of TLR2 activation with chronic respiratory disease suggests its significant role in the T-assisted immune response in COPD, offering a new treatment approach for COPD with lung infections<sup>39,40</sup>. Hausmann et al.<sup>41</sup> found that TLR2 expression was increased in the intestinal mucosa of CD patients using immunohistochemistry and RT-

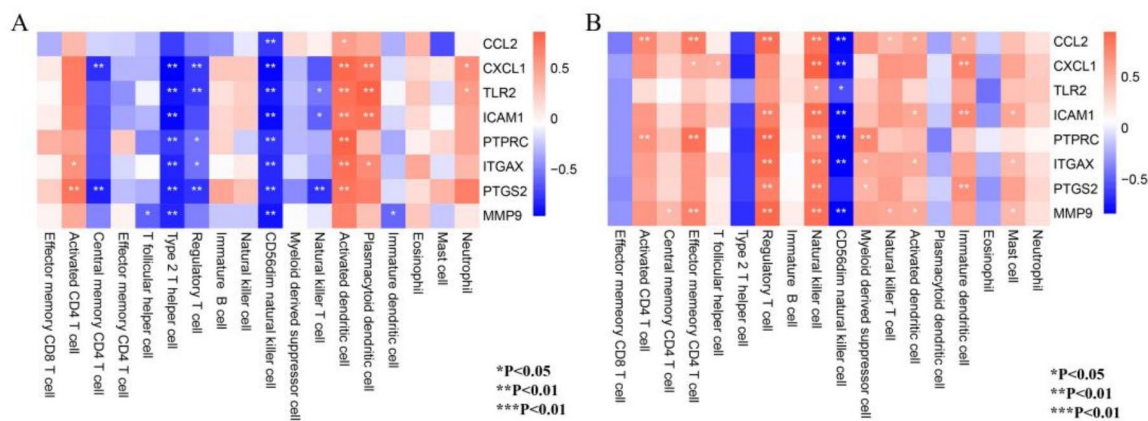


**Fig. 11.** Relationship between hub genes and immune cell infiltration in COPD and CD. (A) Heatmap of correlation analysis in COPD. (B) Heatmap of correlation analysis in CD.

pert_type	pert_id	pert_iname	raw_cs	fdr_q_nlog10	norm_cs
trt_cp	BRD-K62627508	RG-7388	-0.8358	15.6536	-1.869
trt_cp	BRD-K08547377	Irinotecan	-0.8296	15.6536	-1.8554
trt_cp	BRD-K63343048	Orlistat	-0.8195	15.6536	-1.8326
trt_cp	BRD-K06426971	Ryuvidine	-0.7996	15.6536	-1.7881
trt_cp	BRD-K06593056	LE-135	-0.7994	15.6536	-1.7877
trt_cp	BRD-K59574735	Ubenimex	-0.7893	15.6536	-1.7651
trt_cp	BRD-K17705806	JTC-801	-0.7882	15.6536	-1.7626
trt_cp	BRD-K36007650	Puromycin	-0.7867	15.6536	-1.7593
trt_cp	BRD-K46604138	Dapagliflozin	-0.783	15.6536	-1.751
trt_cp	BRD-K46386702	ARRY-334,543	-0.781	15.6536	-1.7466

**Table 1.** Potential drugs predicted by the CMAP database.

PCR. They observed elevated mRNA expression of TLR2 in macrophages associated with inflammation in CD patients, and immunohistochemistry confirmed a significant rise in TLR2 protein in inflamed mucosa. ICAM1 played a key role in leukocyte transendothelial migration (TEM), which regulated leukocyte rolling and adhesion to the vascular wall and directed leukocytes to penetrate the endothelial layer, thereby causing inflammation<sup>42</sup>. Leukocyte migration and interactions between fibroblasts and inflammatory cells lead to a notable rise in ICAM1 expression in lung fibroblasts of COPD patients<sup>43</sup>. Studies had shown that PTPRC was an important regulator of T-cell and B-cell antigen receptor-mediated activation and was widely involved in the regulation of the immune system, affecting cell proliferation, apoptosis, and signalling pathways<sup>44,45</sup>. ITGAM and ITGAX encoded integrins alphaM and alphaX, forming CR3 and CR4 receptors on leukocytes. These receptors were involved in neutrophil and monocyte adherence to endothelial cells and in the phagocytosis of complement-coated particles<sup>46</sup>. Ye et al.<sup>47</sup> found that PTGS2 might be a potential diagnostic biomarker for CD. In addition, PTGS2 expression was increased in inflamed mucosa of CD patients, activating the prostaglandin D2 (PGD2) metabolic pathway<sup>48</sup>. The study by Wang et al.<sup>49</sup> revealed the association between reduced SFTPB expression and the inflammatory response in COPD, which may promote PTGS2 expression and further inflammation. A study by Wells et al.<sup>50</sup> found that elevated MMP9 levels were associated with an increased risk of acute exacerbation of COPD. An imbalance between MMP9 and TIMP1 levels could lead to abnormal ECM degradation or accumulation of ECM proteins in alveolar and small airway walls, potentially contributing to COPD development<sup>51</sup>. Thus, CCL2, TLR2, ICAM1, PTPRC, ITGAX, PTGS2, and MMP9 molecules played

important roles in both inflammatory response and immune regulation in COPD and CD, which was consistent with the results of this study. Despite identifying shared genetic markers through bioinformatics, the specific mechanisms of action in the gut-lung axis were not fully understood. Further studies were required to clarify the interactions and relationships among these molecular markers in the gut-lung axis. Tang et al.<sup>21</sup> demonstrated the regulatory effect of gut microbiota on lung diseases via the gut-lung axis. Short-chain fatty acids, particularly butyrate, produced by gut bacteria, inhibited the mevalonate pathway and potentially reduced lung damage in chronic obstructive pulmonary disease (COPD) by modulating the systemic innate immune response<sup>52,53</sup>. Animal studies, as referenced in the work by Dickson et al.<sup>54</sup>, have demonstrated that alterations to the gut microbiota through antibiotics or dietary modifications can significantly influence allergic airway inflammation triggered by CD4 T cells in the host. Numerous data suggested that short-chain fatty acids played an important immunomodulatory function in peripheral tissues through the regulation of the gut-lung axis<sup>55–57</sup>. Therefore, gut microbiome interventions were another promising target for improving lung disease, which was consistent with the evidence provided in this study for COPD and CD.

The immune infiltration of eight hub genes suggested that intestinal diseases might affect the respiratory system and trigger respiratory immunity through specific immune cells. Further experiments were required to confirm this hypothesis. Analysis of the top 10 up- and down-regulated genes in both diseases using the CMap database revealed small molecule drugs associated with the expression of these shared genes. In particular, Dapagliflozin can regulate the composition and abundance of intestinal microbes, impacting intestinal function<sup>58</sup>. Studies had shown that Orlistat altered the metabolic activity of gut microorganisms by inhibiting the activity of gastrointestinal lipases, which further affected the inflammatory response and barrier function of intestinal epithelial cells<sup>59</sup>.

The study's limitations stemmed from its limited sample size. Among the eight hub genes identified, only ITGAX and TLR2 showed differential expression in the COPD external validation dataset, with TLR2 being overexpressed in two datasets, which may limit its biomarker potential. Nonetheless, the diagnostic and prognostic significance of these core genes was confirmed using an independent dataset, which bolsters the reliability of our findings. Future experimental validation was crucial for confirming these results. Challenges persist in fully understanding disease mechanisms despite insights gained from gene and pathway analyses. To precisely elucidate the complex relationships between COPD, CD, and their phenotypes, expanding the sample size and conducting diverse studies are necessary.

## Materials and methods

The design flowchart of the study was shown in Fig. 12.

### Data collection

Gene expression for (chronic obstructive pulmonary disease) COPD and Crohn's disease (CD) was downloaded from the GEO (<http://www.ncbi.nlm.nih.gov/geo/>) database. COPD GSE148004 was an independent dataset that included tissues from 7 COPD patients and 9 healthy individuals. The independent dataset GSE75214 included 8 CD tissues and 11 healthy tissues. The COPD validation dataset GSE55962 contained tissues from 24 COPD tissues and 82 normal controls, and GSE112811 contained tissues from 20 COPD tissues and 44 normal controls. The CD validation dataset GSE102133 contained tissues from 62 CD tissues and 12 normal controls.

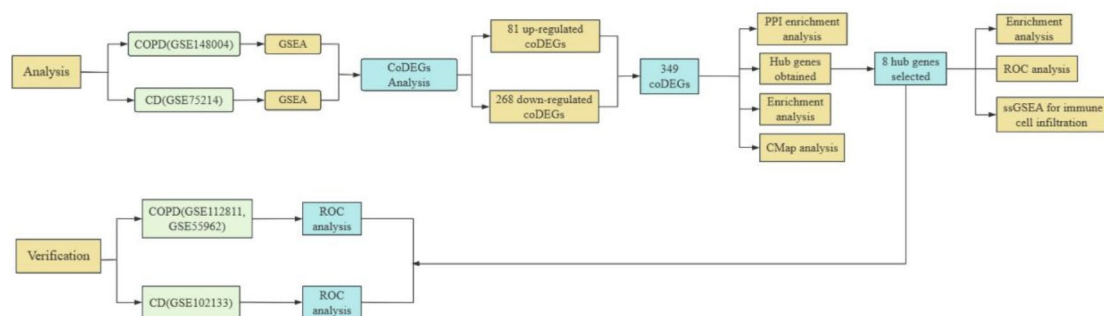


**Fig. 12.** Flow chart of research design.

(Supplementary Table 1). After obtaining the gene expression data, gene annotation was performed using R software (version 4.3.2, June 11, 2024).

### Gene set enrichment analysis in COPD and CD

Gene set enrichment analysis (GSEA) was conducted for COPD and CD using the ClusterProfiler package in R software (version 4.3.2, June 16, 2024). The analysis utilized the gseKEGG function with specific parameters: minGSSize = 3, maxGSSize = 500, pvalueCutoff = 0.05, and pAdjustMethod = 'BH'.

### Identification of differentially expressed genes in COPD and CD

The GEO database data was normalized using the 'limma' package in R software (version 4.3.2, June 11, 2024). We found that when COPD and CD were selected  $|\log_2(\text{FoldChange})| > 0.5$  or  $|\log_2(\text{FoldChange})| > 1.0$ , the subsequent analyses were unsatisfactory. Therefore, screening criteria for COPD differentially expressed genes were: adjusted p-value  $< 0.05$  (p.adj  $< 0.05$ ) and  $|\log_2(\text{FoldChange})| > 1$ , and for CD differentially expressed genes: adjusted p-value  $< 0.05$  (p.adj  $< 0.05$ ) and  $|\log_2(\text{FoldChange})| > 0.5$ . Volcano plots visualized the DEGs for COPD and CD, created using the 'ggplot2' package in R software (version 4.3.2, June 11, 2024). Common DEGs for up and down regulation in COPD and CD were termed up coDEGs and down coDEGs. The overlap of the DEGs between the two diseases was identified by drawing "ComplexHeatmap" and "VennDiagram" using bioinformatics tools on the Xiantao academic website (<https://www.xiantaozi.com/>).

### Functional enrichment analysis

Gene ontology (GO) and Kyoto Encyclopedia of Genes and Genomes (KEGG) enrichment analyses were performed on selected coDEGs using the R ClusterProfiler package. Statistically significant coDEGs were identified with thresholds of qvalue  $< 0.01$ , pvalue  $< 0.05$ , and pAdjustMethod = 'BH'.

### Constructing protein-protein interaction networks to access key modules and hub genes

The STRING database (<https://string-db.org/>) was used to perform searches for molecular interactions and to predict protein interactions. The protein-protein interaction (PPI) network of 349 coDEGs in COPD and CD were constructed by setting the reference value to a confidence score greater than 0.4. The PPI network graphs were further visualised with the help of Cytoscape (version 3.9.1) software. The Molecular Complex Detection (MCODE) plug-in in Cytoscape was used to screen the core gene clusters for PPI interactions in coDEGs. The screening criteria for the key modules included MCODE degree cutoff  $> 2$ , node score cutoff = 0.2, maximum depth = 100, and k-score = 2. The maximum correlation (MCC) algorithm, maximum neighbourhood component (MNC) algorithm, degree algorithm, and edge penetration component (EPC) algorithm were used to filter core gene clusters from 349 coDEGs using the CytoHubba plug-in in Cytoscape software. Subsequently, the pivotal genes were screened using the Xiantao academic website.

### Enrichment analysis, expression level verification and diagnostic value of hub genes

GO and KEGG enrichment analysis of hub genes was performed using the ClusterProfiler package and the results were visualised using the ggplot2 package. Receiver operating characteristic (ROC) curves were plotted to assess the diagnostic value of the centromeric genes using the qROC package in R software (version 4.3.2, June 29, 2024). Area under the curve (AUC) and 95% confidence interval (CI) were used to assess the levels of hub genes on COPD and CD, respectively. In addition, the shared hub genes were externally validated using the validation datasets GSE112811, GSE55962, and GSE102133, and the expression levels of the diagnostic biomarker genes were further validated by performing the Mann-Whitney U test (Wilcoxon rank-sum test) for the hub genes based on the expression profile data characteristics.

### Immune cell infiltration analysis

By using Single Sample Gene Set Enrichment Analysis (ssGSEA) in the GSVA package, this study aimed to validate bioinformatics results and explore the link between COPD and CD. The study calculated infiltration levels of 28 immune cells in COPD and CD gene sets, focusing on 18 specific immune cells. Data on immune cells and immune function were combined to create heat maps with immune cell clustering. Box plots were generated using the ggplot2 package in R software (version 4.3.2, July 5, 2024) to compare expression levels of immune cells in disease and control samples. The Wilcoxon rank sum test was used to identify statistically significant differences ( $P < 0.05$ ). Correlation coefficients and P-values were calculated for pivotal genes and immune cell abundance profiles, with P-values  $< 0.05$  considered significant. A heatmap showing the correlation between immune cells and pivotal genes was created using the pheatmap package in R software (version 4.3.2, July 5, 2024).

### CMap database for drug response prediction studies on the basis of common genes

Connectivity Map (CMap) (<https://clue.io/query>) was a gene expression profiling database used to identify potential therapeutic targets or drugs submitted to gene signatures. 10 up regulated genes and 10 down regulated genes were loaded into the CMap online tool. The proximity between the query signature and the compound was estimated using the score from norm\_cs. Drugs with negative scores were usually interpreted as having potential therapeutic effects and will be selected as drug candidates.

### Conclusion

In this study, the common molecular pathogenesis of COPD and CD was investigated, revealing their connection through the gut-lung axis. The study found that COPD and CD could interact through the innate and adaptive immune systems. Analysis of immune infiltration identified eight hub genes involved in the immunopathological

processes of both diseases. This offered new insights into their pathogenesis, molecular mechanisms increasing their morbidity, and potential therapeutic targets. Using CMAP to predict potential drugs enhanced our understanding of these diseases and offered new avenues for therapeutic strategies.

## Data availability

The original data used in this study are all publicly available. This data can be found here: <https://www.ncbi.nlm.nih.gov/geo/> under the accession numbers GSE148004, GSE75214, GSE55962, GSE112811, and GSE102133. My data is provided within the supplementary information files.

Received: 4 September 2024; Accepted: 4 November 2024

Published online: 10 November 2024

## References

- Chen, S. et al. The global economic burden of chronic obstructive pulmonary disease for 204 countries and territories in 2020–50: a health-augmented macroeconomic modelling study. *Lancet Glob. Health.* **11**(8), e1183–e1193. [https://doi.org/10.1016/s2214-109x\(23\)00217-6](https://doi.org/10.1016/s2214-109x(23)00217-6) (2023).
- Labaki, W. W. & Rosenberg, S. R. Chronic obstructive pulmonary disease. *Ann. Intern. Med.* **3**, ITC17–ITC32. <https://doi.org/10.7326/aitc202008040> (2020).
- Soriano, J. B. et al. Global, regional, and national deaths, prevalence, disability-adjusted life years, and years lived with disability for chronic obstructive pulmonary disease and asthma, 1990–2015: a systematic analysis for the global burden of Disease Study 2015. *Lancet Respir. Med.* **9**, 691–706. [https://doi.org/10.1016/s2213-2600\(17\)30293-x](https://doi.org/10.1016/s2213-2600(17)30293-x) (2017).
- Cao, Y., Pan, H., Yang, Y., Zhou, J. & Zhang, G. Screening of potential key ferroptosis-related genes in chronic obstructive pulmonary disease. *Int. J. Chronic Obstr. Pulm. Dis.* **18**, 2849–2860. <https://doi.org/10.2147/copd.S422835> (2023).
- Ortiz-Quintero, B., Martínez-Espinosa, I. & Pérez-Padilla, R. Mechanisms of lung damage and development of COPD due to household biomass-smoke exposure: inflammation, oxidative stress, MicroRNAs, and gene polymorphisms. *Cells.* **12** (1), 67 (2022).
- Dalle, S. & Koppo, K. Is inflammatory signaling involved in disease-related muscle wasting? Evidence from osteoarthritis, chronic obstructive pulmonary disease and type II diabetes. *Exp. Gerontol.* <https://doi.org/10.1016/j.exger.2020.110964> (2020).
- Li, C. L. & Liu, S. F. Exploring molecular mechanisms and biomarkers in COPD: an overview of current advancements and perspectives. *Int. J. Mol. Sci.* **25** (13). <https://doi.org/10.3390/ijms25137347> (2024).
- Wrench, C. L. et al. Small airway fibroblasts from patients with chronic obstructive pulmonary disease exhibit cellular senescence. *Am. J. Physiol.-Lung Cell. Mol. Physiol.* **326** (3), L266–L279 (2024).
- Bu, T., Wang, L. F. & Yin, Y. Q. How do innate immune cells contribute to airway remodeling in COPD progression? *Int. J. Chronic Obstr. Pulm. Dis.* **15** 107–116. <https://doi.org/10.2147/copd.S235054> (2020).
- He, Y. et al. Gut–lung axis: the microbial contributions and clinical implications. *Crit. Rev. Microbiol.* **43** (1), 81–95. <https://doi.org/10.1080/1040841x.2016.1176988> (2016).
- Laass, M. W., Roggenbuck, D. & Conrad, K. Diagnosis and classification of Crohn's disease. *Autoimmun. rev.* **13** (4–5), 467–471. <https://doi.org/10.1016/j.autrev.2014.01.029> (2014).
- Sands, B. E. From symptom to diagnosis: clinical distinctions among various forms of intestinal inflammation. *Gastroenterology.* **126** (6), 1518–1532. <https://doi.org/10.1053/j.gastro.2004.02.072> (2004).
- Jarmakiewicz-Czajka, S., Gruszecka, J. & Filip, R. The diagnosis of intestinal fibrosis in Crohn's disease—present and future. *Int. J. Mol. Sci.* **25** (13). <https://doi.org/10.3390/ijms25136935> (2024).
- Santana, P. T., Rosas, S. L. B., Ribeiro, B. E., Marinho, Y. & de Souza, H. S. P. Dysbiosis in inflammatory bowel disease: pathogenic role and potential therapeutic targets. *Int. J. Mol. Sci.* <https://doi.org/10.3390/ijms23073464> (2022).
- Torres, J., Mehandru, S., Colombel, J. F. & Peyrin-Biroulet, L. Crohn's disease. *Lancet.* **389**(10080), 1741–1755. [https://doi.org/10.1016/s0140-6736\(16\)31711-1](https://doi.org/10.1016/s0140-6736(16)31711-1) (2017).
- Enaud, R. et al. The gut-lung Axis in Health and Respiratory diseases: a place for inter-organ and Inter-kingdom Crosstalks. *Front. Cell. Infect. Microbiol.* <https://doi.org/10.3389/fcimb.2020.00009> (2020).
- Jess, T. Survival and cause specific mortality in patients with inflammatory bowel disease: a long term outcome study in Olmsted County, Minnesota, 1940–2004. *Gut.* **55**(9), 1248–1254. <https://doi.org/10.1136/gut.2005.079350> (2006).
- Raj, A. A. et al. Prevalence of inflammatory bowel disease in patients with airways disease. *Respir. Med.* **102** (5), 780–785. <https://doi.org/10.1016/j.rmed.2007.08.014> (2008).
- Pemmasani, G., Loftus, E. V. & Tremaine, W. J. Prevalence of pulmonary diseases in association with inflammatory bowel disease. *Dig. Dis. Sci.* **67** (11), 5187–5194. <https://doi.org/10.1007/s10620-022-07385-z> (2022).
- Cheng, Z. X. & Zhang, J. Exploring the role of Gut–Lung interactions in COPD Pathogenesis: a comprehensive review on microbiota characteristics and inflammation modulation. *Chronic Obstr. Pulm. Dis. J. COPD Found.* **11** (3), 311–325. <https://doi.org/10.15326/jcopdf.2023.0442> (2024).
- Tang, J., Xu, L., Zeng, Y. & Gong, F. Effect of gut microbiota on LPS-induced acute lung injury by regulating the TLR4/NF-kB signaling pathway. *Int. Immunopharmacol.* **91**, 107272 (2021).
- Budden, K. F. et al. Emerging pathogenic links between microbiota and the gut–lung axis. *Nat. Rev. Microbiol.* **15** (1), 55–63. <https://doi.org/10.1038/nrmicro.2016.142> (2016).
- Mahmud, S. M., Hasan., Al-Mustanjid, M., Akter, F., Rahman, M. S. & Ahmed, K. Bioinformatics and system biology approach to identify the influences of SARS-CoV-2 infections to idiopathic pulmonary fibrosis and chronic obstructive pulmonary disease patients. *Brief. Bioinform.* **22** (5). <https://doi.org/10.1093/bib/bbab115> (2021).
- Huang, R. et al. Identifying immune cell infiltration and effective diagnostic biomarkers in Crohn's disease by bioinformatics analysis. *Front. Immunol.* **14**, 1162473. <https://doi.org/10.3389/fimmu.2023.1162473> (2023).
- Halbert, R. J. et al. Global burden of COPD: systematic review and meta-analysis. *Eur. Respir. J.* **28**(3), 523–532. <https://doi.org/10.1183/09031936.06.00124605> (2006).
- Zhu, E. et al. Screening of immune-related secretory proteins linking chronic kidney disease with calcific aortic valve disease based on comprehensive bioinformatics analysis and machine learning. *J. Transl. Med.* **21** (1). <https://doi.org/10.1186/s12967-023-04171-x> (2023).
- Wang, Y. et al. Exploring the common mechanism of vascular dementia and inflammatory bowel disease: a bioinformatics-based study. *Front. Immunol.* <https://doi.org/10.3389/fimmu.2024.1347415> (2024).
- Shi, H., Zhao, T., Geng, R., Sun, L. & Fan, H. The associations between gut microbiota and chronic respiratory diseases: a mendelian randomization study. *Front. Microbiol.* <https://doi.org/10.3389/fmicb.2023.1200937> (2023).
- Slyepchenko, A. et al. Intestinal dysbiosis, Gut Hyperpermeability and bacterial translocation: missing links between depression, obesity and type 2 diabetes. *Curr. Pharm. Des.* **22**(40), 6087–6106. <https://doi.org/10.2174/1381612822666160922165706> (2016).
- Samuelson, D. R., Welsh, D. A. & Shellito, J. E. Regulation of lung immunity and host defense by the intestinal microbiota. *Front. Microbiol.* <https://doi.org/10.3389/fmicb.2015.01085> (2015).

31. Lai, H. C. et al. Gut microbiota modulates COPD pathogenesis: role of anti-inflammatory parabacteroides goldsteinii lipopolysaccharide. *Gut*. **71**(2), 309–321. <https://doi.org/10.1136/gutjnl-2020-322599> (2022).
32. Yang, R. et al. Drug-induced senescence by aurora kinase inhibitors attenuates innate immune response of macrophages on gastric cancer organoids. *Cancer Lett.* <https://doi.org/10.1016/j.canlet.2024.217106> (2024).
33. Sun, C. et al. MCP-1/CCR-2 axis in adipocytes and cancer cell respectively facilitates ovarian cancer peritoneal metastasis. *Oncogene*. **39**(8), 1681–1695. <https://doi.org/10.1038/s41388-019-1090-1> (2019).
34. Dong, Y. et al. Targeting CCL2-CCR2 signaling pathway alleviates macrophage dysfunction in COPD via PI3K-AKT axis. *Cell. Communication Signal.* <https://doi.org/10.1186/s12964-024-01746-z> (2024).
35. Ranjbar, M., Rahimi, A., Baghernejadan, Z., Ghorbani, A. & Khorramdelazad, H. Role of CCL2/CCR2 axis in the pathogenesis of COVID-19 and possible treatments: all options on the table. *Int. Immunopharmacol.* <https://doi.org/10.1016/j.intimp.2022.109325> (2022).
36. Giri, J., Das, R., Nylen, E., Chinnadurai, R. & Galipeau, J. CCL2 and CXCL12 derived from mesenchymal stromal cells cooperatively polarize IL-10 + tissue macrophages to Mitigate Gut Injury. *Cell. Rep.* **30**(6), 1923–1934.e1924 <https://doi.org/10.1016/j.celrep.2020.01.047> (2020).
37. Korbecki, J., Barczak, K., Gutowska, I., Chlubek, D. & Baranowska-Bosiacka, I. CXCL1: Gene, promoter, regulation of expression, mRNA stability, regulation of activity in the intercellular space. *Int. J. Mol. Sci.* <https://doi.org/10.3390/ijms23020792> (2022).
38. Barnes, P. J. Inflammatory mechanisms in patients with chronic obstructive pulmonary disease. *J. Allergy Clin. Immunol.* **138** (1), 16–27. <https://doi.org/10.1016/j.jaci.2016.05.011> (2016).
39. Lou, Y. & Jiang, G. Associations between TLRs 2 and 4, and  $\beta$ -lactam antibiotics in COPD patients complicated with pulmonary infections. *J. Infect. Dev. Ctries.* **18** (06), 950–956. <https://doi.org/10.3855/jidc.18918> (2024).
40. Sidletskaya, K., Vitkina, T., & Denisenko, Y. The role of toll-like receptors 2 and 4 in the pathogenesis of chronic obstructive pulmonary disease. *Int. J. Chronic Obstruct. Pulm. Dis.* **15**, 1481–1493 <https://doi.org/10.2147/copd.S249131> (2020).
41. Hausmann, M., Kiessling, S., Mestermann, S., Webb, G., Spöttl, T., Andus, T., Schölmerich, J., Herfarth, H., Ray, K., Falk, W., & Rogler, G. Toll-like receptors 2 and 4 are up regulated during intestinal inflammation. *Gastroenterology*. **122**(7), 1987–2000. <https://doi.org/10.1053/gast.2002.33662> (2002).
42. Bui, T. M., Wiesolek, H. L., & Sumagin, R. ICAM-1: a master regulator of cellular responses in inflammation, injury resolution, and tumorigenesis. *J. Leukocyte Biol.* **108**(3), 787–799. <https://doi.org/10.1002/jlb.2mr0220-549r> (2020).
43. Zandvoort, A. High ICAM-1 gene expression in pulmonary fibroblasts of COPD patients: a reflection of an enhanced immunological function. *Eur. Respir. J.* **28**(1), 113–122. <https://doi.org/10.1183/09031936.06.00116205> (2006).
44. Li, X., Yue, Z., Wang, D., & Zhou, L. PTPRC functions as a prognosis biomarker in the tumor microenvironment of cutaneous melanoma. *Sci. Rep.* <https://doi.org/10.1038/s41598-023-46794-6> (2023).
45. Al Barashdi, M. A., Ali, A., McMullin, M. F., & Mills, K. Protein tyrosine phosphatase receptor type C (PTPRC or CD45). *J. Clin. Pathol.* **74**(9), 548–552. <https://doi.org/10.1136/jclinpath-2020-206927> (2021).
46. Shi, D., Zhong, Z., Xu, R., Li, B., Li, J., Habib, U., Peng, Y., Mao, H., Li, Z., Huang, F., Yu, X., & Li, M. Association of ITGAX and ITGAM gene polymorphisms with susceptibility to IgA nephropathy. *J. Hum. Genet.* **64**(9), 927–935. <https://doi.org/10.1038/s10038-019-0632-2> (2019).
47. Ye, C., Zhu, S., & Yuan, J. Construction of ceRNA Network to reveal potential biomarkers in Crohn's disease and validation in a TNBS induced mice model. *J. Inflamm. Res.* **14**, 6447–6459. <https://doi.org/10.2147/jir.S338053> (2021).
48. Le Loupp, A.-G., Bach-Ngohou, K., Bourreille, A., Boudin, H., Rolli-Derkinderen, M., Denis, M. G., Neunlist, M., & Masson, D. Activation of the prostaglandin D2 metabolic pathway in Crohn's disease: involvement of the enteric nervous system. *BMC Gastroenterol.* <https://doi.org/10.1186/s12876-015-0338-7> (2015).
49. Wang, Y., Gao, X., Li, Y., Wang, X., Li, Y., Zhang, S., Liu, H., Guo, H., Lu, W., & Sun, D. Pulmonary surfactant-associated protein B regulates prostaglandin-endoperoxide synthase-2 and inflammation in chronic obstructive pulmonary disease. *Exp. Physiol.* **106**(5), 1303–1311. <https://doi.org/10.1113/ep089244> (2021).
50. Wells, J. M., Parker, M. M., Oster, R. A., Bowler, R. P., Dransfield, M. T., Bhatt, S. P., Cho, M. H., Kim, V., Curtis, J. L., Martinez, F. J., Paine, R., O'Neal, W., Labaki, W. W., Kaner, R. J., Barjaktarevic, I., Han, M. K., Silverman, E. K., Crapo, J. D., Barr, R. G. Elevated circulating MMP-9 is linked to increased COPD exacerbation risk in SPIROMICS and COPD Gene. *JCI Insight.* <https://doi.org/10.1172/jci.insight.123614> (2018).
51. Li, S., Li, Y., Lu, Y., Zhao, Z., Wang, J., Li, J., Wang, W., & Song, L. Relationships of MMP-9 and TIMP-1 proteins with chronic obstructive pulmonary disease risk: a systematic review and meta-analysis. *J. Res. Med. Sci.* <https://doi.org/10.4103/1735-1995.178737> (2016).
52. Ding, K., Chen, J., Zhan, W., Zhang, S., Chen, Y., Long, S., & Lei, M. Microbiome links cigarette smoke-induced chronic obstructive pulmonary disease and dietary fiber via the gut-lung axis: a narrative review. *COPD J. Chronic Obstruct. Pulm. Dis.* **19**(1), 10–17. <https://doi.org/10.1080/15412555.2021.2019208> (2021).
53. Hopkins, R. J., & Young, R. P. Mevalonate signaling, COPD and cancer: the statins and beyond. *J. Investig. Med.* **67**(4), 711–714. <https://doi.org/10.1136/jim-2018-000829> (2023).
54. Dickson, R. P., Erb-Downward, J. R., Martinez, F. J., & Huffnagle, G. B. The microbiome and the respiratory tract. *Annu. Rev. Physiol.* **78**(1), 481–504. <https://doi.org/10.1146/annurev-physiol-021115-105238> (2016).
55. Dang, A. T., & Marsland, B. J. Microbes, metabolites, and the gut–lung axis. *Mucosal Immunol.* **12**(4), 843–850. <https://doi.org/10.1038/s41385-019-0160-6> (2019).
56. Maslowski, K. M., Vieira, A. T., Ng, A., Kranich, J., Sierro, F., Di, Y., Schilter, H. C., Rolph, M. S., Mackay, F., Artis, D., Xavier, R. J., Teixeira, M. M., & Mackay, C. R. Regulation of inflammatory responses by gut microbiota and chemoattractant receptor GPR43. *Nature*. **461**(7268), 1282–1286. <https://doi.org/10.1038/nature08530> (2009).
57. Trompette, A., Gollwitzer, E. S., Yadava, K., Sichelstiel, A. K., Sprenger, N., Ngom-Bru, C., Blanchard, C., Junt, T., Nicod, L. P., Harris, N. L., & Marsland, B. J. Gut microbiota metabolism of dietary fiber influences allergic airway disease and hematopoiesis. *Nat. Med.* **20**(2), 159–166. <https://doi.org/10.1038/nm.3444> (2014).
58. Bao, N., Liu, X., Zhong, X., Jia, S., Hua, N., Zhang, L., & Mo, G. Dapagliflozin-affected endothelial dysfunction and altered gut microbiota in mice with heart failure. *PeerJ.* <https://doi.org/10.7717/peerj.15589> (2023).
59. Katimbwa, D. A., Oh, J., Jang, C. H., & Lim, J. Orlistat, a competitive lipase inhibitor used as an antiobesity remedy, enhances inflammatory reactions in the intestine. *Appl. Biol. Chem.* <https://doi.org/10.1186/s13765-022-00712-y> (2022).

## Acknowledgements

This project was funded by the Jiangsu Province Chinese Medicine Science and Technology Development Program Project Face-up Project (MS2023178), the Lianyungang Traditional Chinese Medicine science and technology development plan project (ZD202203) and Lianyungang Traditional Chinese Medicine science and technology project (LZYZD202403).

## Author contributions

Z.X.: Writing—original draft, software, investigation, formal analysis, data curation, conceptualization. L.C.: Writing—original draft, investigation, visualization, software, data curation. C.L.: Writing—original draft, vis-

ualization, validation, software, investigation. T.H.: Writing—original draft, visualization, software, validation, data curation. J.H.: Writing—original draft, investigation, software, validation, data curation. H.C.: Writing—original draft, validation, software, investigation. D.X.: Writing—original draft, visualization, validation, investigation. Z.F.: Writing—original draft, validation, investigation. Q.K.: Writing—original draft, visualization. L.Q.: Writing—original draft, software. S.J.: Methodology, investigation, formal analysis, writing—original draft, writing—review and editing. Z.Y.: Writing—original draft, validation, supervision, resources, project administration. J.S.: Methodology, investigation, formal analysis, writing—original draft, writing—review and editing. Y.Z.: Writing—original draft, validation, supervision, resources, project administration.

## Declarations

### Competing interests

The authors declare no competing interests.

### Additional information

**Supplementary Information** The online version contains supplementary material available at <https://doi.org/10.1038/s41598-024-78697-5>.

**Correspondence** and requests for materials should be addressed to J.S. or Y.Z.

**Reprints and permissions information** is available at [www.nature.com/reprints](http://www.nature.com/reprints).

**Publisher's note** Springer Nature remains neutral with regard to jurisdictional claims in published maps and institutional affiliations.

**Open Access** This article is licensed under a Creative Commons Attribution-NonCommercial-NoDerivatives 4.0 International License, which permits any non-commercial use, sharing, distribution and reproduction in any medium or format, as long as you give appropriate credit to the original author(s) and the source, provide a link to the Creative Commons licence, and indicate if you modified the licensed material. You do not have permission under this licence to share adapted material derived from this article or parts of it. The images or other third party material in this article are included in the article's Creative Commons licence, unless indicated otherwise in a credit line to the material. If material is not included in the article's Creative Commons licence and your intended use is not permitted by statutory regulation or exceeds the permitted use, you will need to obtain permission directly from the copyright holder. To view a copy of this licence, visit <http://creativecommons.org/licenses/by-nc-nd/4.0/>.

© The Author(s) 2024